Commun Nonlinear Sci Numer Simulat 38 (2016) 117–129

Contents lists available at ScienceDirect

Commun Nonlinear Sci Numer Simulat

journal homepage: www.elsevier.com/locate/cnsns

Earthquake nucleation in a stochastic fault model of globally coupled units with interaction delays

Nebojša Vasović[a], Srđan Kostić[b,*], Igor Franović[c], Kristina Todorović[d]

[a] Department of Applied Mathematics, Faculty of Mining and Geology, University of Belgrade, Serbia
[b] Institute for Development of Water Resources "Jaroslav Černi", Jaroslava Černog 80, 11226 Belgrade, Serbia
[c] Scientific Computing Lab, Institute of Physics, University of Belgrade, Serbia
[d] Department of Physics and Mathematics, Faculty of Pharmacy, University of Belgrade, Serbia

ARTICLE INFO

Article history:
Received 6 March 2015
Revised 9 December 2015
Accepted 7 February 2016
Available online 26 February 2016

Keywords:
Time delay
Seismic noise
Bifurcation
Bistability

ABSTRACT

In present paper we analyze dynamics of fault motion by considering delayed interaction of 100 all-to-all coupled blocks with rate-dependent friction law in presence of random seismic noise. Such a model sufficiently well describes a real fault motion, whose prevailing stochastic nature is implied by surrogate data analysis of available GPS measurements of active fault movement. Interaction of blocks in an analyzed model is studied as a function of time delay, observed both for dynamics of individual faults and phenomenological models. Analyzed model is examined as a system of all-to-all coupled blocks according to typical assumption of compound faults as complex of globally coupled segments. We apply numerical methods to show that there are local bifurcations from equilibrium state to periodic oscillations, with an occurrence of irregular aperiodic behavior when initial conditions are set away from the equilibrium point. Such a behavior indicates a possible existence of a bi-stable dynamical regime, due to effect of the introduced seismic noise or the existence of global attractor. The latter assumption is additionally confirmed by analyzing the corresponding mean-field approximated model. In this bi-stable regime, distribution of event magnitudes follows Gutenberg–Richter power law with satisfying statistical accuracy, including the b-value within the real observed range.

1. Introduction

Burridge–Knopoff (BK) model is commonly recognized as a phenomenological model of earthquake fault motion. Since the original experiment of Burridge and Knopoff [1], an array of interconnected blocks driving along the rough surface has been used to mimic the seismic movement along a fault, whose dynamics was repeatedly proved to obey Gutenberg–Richter and Omori–Utsu law [1–7]. Two different models are typically analyzed in this case: discrete one-dimensional or two-dimensional BK model and cellular automata version, initially proposed by Olami et al. [8]. Both of these models are equally used in observing the qualitative features of seismic fault motion [9–12]. Except for the seismic features arising from the specific friction law at the contact of blocks and rough surface of the lower plate [1,13–15] and from the viewpoint of statistical physics [16], BK model and its different variants have been studied from the viewpoint of nonlinear dynamics. Practically, dynamical instabilities in BK model have been studied mainly for single-and two-block models. Apparently, symmetric two-block models can produce spatially asymmetric dynamics [17]. On the other hand, asymmetric models, e.g. with different

* Corresponding author. Tel.: +381 642848406.
E-mail address: srdjan.kostic@jcerni.co.rs (S. Kostić).

http://dx.doi.org/10.1016/j.cnsns.2016.02.011
1007-5704/

friction forces on each block, exhibit deterministic chaos for certain parameter ranges [18]. Field et al. [19] analyzed an electronic analog of a two-block mechanical system, and found very rich dynamics as a function of coupling strength. Indeed, their results indicate that the circuit exhibits alternating regions of periodic and chaotic behavior as coupling strength is varied. Galvanetto [20] studied the two-block BK model and showed that several periodic, quasi-periodic and chaotic attractors can coexist in this simple system. Erickson et al. [21] analyzed dynamics of one-block BK model with Dieterich–Ruina friction law and found that system undergoes a Hopf bifurcation to a periodic orbit, which then undergoes a period doubling cascade into a strange attractor. Similarly, the same authors [22] analyzed the dynamics of one-dimensional BK model, and showed that it also exhibits both periodic and chaotic motions, but with the size-dependent system's transition to chaos. Within this research, we also analyze behavior of one-dimensional BK model from the viewpoint of nonlinear dynamics.

One should note that all of these previous studies on the dynamics of BK model analyzed the motion of an array of blocks as a deterministic system, without any stochastic variable. However, if we take into account the fact that the real observed fault motion is stochastic by nature, the starting BK model becomes stochastic, which further excludes the possible occurrence of deterministic chaos. Such a stochasticity naturally arises due to existence of random uncorrelated seismic noise, which originates from small-scale faulting, different irregularities and inhomogeneities or it is of undefined origin [23,24]. For this reason, in present paper we analyze dynamics of BK model in presence of random noise. Nevertheless, it is necessary to emphasize that coherent noise is hardly expected to occur at the seismogenic depth, since it typically arises from the reflection of seismic waves, ground rolls, traffic noise, etc.

Besides the neglected effect of seismic noise on dynamics of fault motion, preceding research on this topic included only the nearest-neighbor coupling in BK model, with only few studies on variable range interaction, primarily from the viewpoint of statistical physics [7,12]. However, long-range interactions are also observed in natural conditions. If we take San Andreas fault system as an example, Sanders [25] suggested that deformation of the northern part of San Jacinto fault zone affects the deformation on the Mojave segment of the San Andreas fault zone, due to geometric continuity of these two fault zones near their intersection. In particular, San Jacinto zone exhibits a seismic cycle every 150 years, which is similar to 132 years of seismic cycle for Mojave segment of San Andreas zone, which could imply that the concentrated stress increase along San Jacinto zone could help induce rupture of the Mojave segment on a similar time scale. If we follow the same reasoning as in Sanders [25], due to geometric continuity among adjacent parts of different segments of San Andreas fault, we could assume that deformation along one fault segment affects deformation along other parts of the same fault, since Johnson and Segall [26] reported that recurrence time of the northern part of San Andreas fault is in the range 188–315 years, close to 132 years for Mojave segment. Now, if we take a look at great earthquakes recorded along the San Andreas fault, namely M7.7 from 1680 in Salton Trough, M7.9 from 1857 in Fort Tejon and M7.8 from 1906 in San Francisco, we could conclude there is an average recurrence period of approximately 150 years between large earthquakes along a single fault. This fact is presumed to confirm two basic assumptions: (1) that all segments of the same fault are indeed in interaction (case of globally coupled units) and (2) that there is a certain delayed effect in their interaction. One should note that, from the viewpoint of nonlinear dynamics, global coupling of blocks represents the limit case of coupling, which is commonly observed in systems with large number of units, like ensembles of neurons [27]. As for the introduced delayed interaction, it could also occur due to assumption of long-range interaction among the units in the observed system, which further implies long-term or memory effect [28]. Practically, if we consider that motion of a single block can represent a seismic event, than it is obvious that such an earthquake would strongly and directly influence the next event, and then the next event again would affect its next one and so on. In other words, movement of a single block or cluster of blocks at time t depends on some preceding motion of connecting blocks at some previous time $t-\tau$. Such an effect is also found to exist in the original work of Burridge and Knopoff [1], who showed that there is a delayed interaction among cluster of blocks, with the intensity of time delay determined by the viscous properties along the specified fault segment. This effect is also qualitatively incorporated in our model by including time delay τ in the connections among blocks of the observed system.

To resume, in present paper we analyze the dynamics of an array of blocks, by assuming all-to-all coupling between them, with a time delay in their interaction and in the presence of seismic noise. Although having real and experimental backgrounds, such a model has not been analyzed so far in previous studies. Our main goal is to examine the qualitative changes of dynamics in a proposed spring-slider model, and to try to explain its origin, with only a phenomenological analogy with the real observed data.

2. Direct evidence of stochastic fault motion

Mechanism of fault motion has been mainly modeled as a deterministic process [for a review, see 16]. Indeed, most deterministic models provide sufficiently accurate results for a phenomenological description of fault motion and earthquake nucleation. This is probably the reason why stochastic models have not been examined so far in this context. Also, there is a lack of direct experimental evidence confirming the stochastic nature of fault motion. Therefore, we firstly investigate the possible stochastic dynamics of fault motion on the basis of experimental data. Since fault motion at seismogenic depths is not accessible for a direct observation, our analysis is based on in situ measurements of ground deformation near active faults, whose dynamics is assumed to sufficiently well mimic the real fault motion. For this purpose, we examine displacement data recorded at 20 different GPS stations, uniformly distributed along the active segments of San Andreas transform fault, as it is shown in Fig. 1 [29]. Analysis was performed using the surrogate data testing of the null hypothesis that data are independent random numbers drawn from some fixed but unknown distribution [30]. Our aim was to achieve a

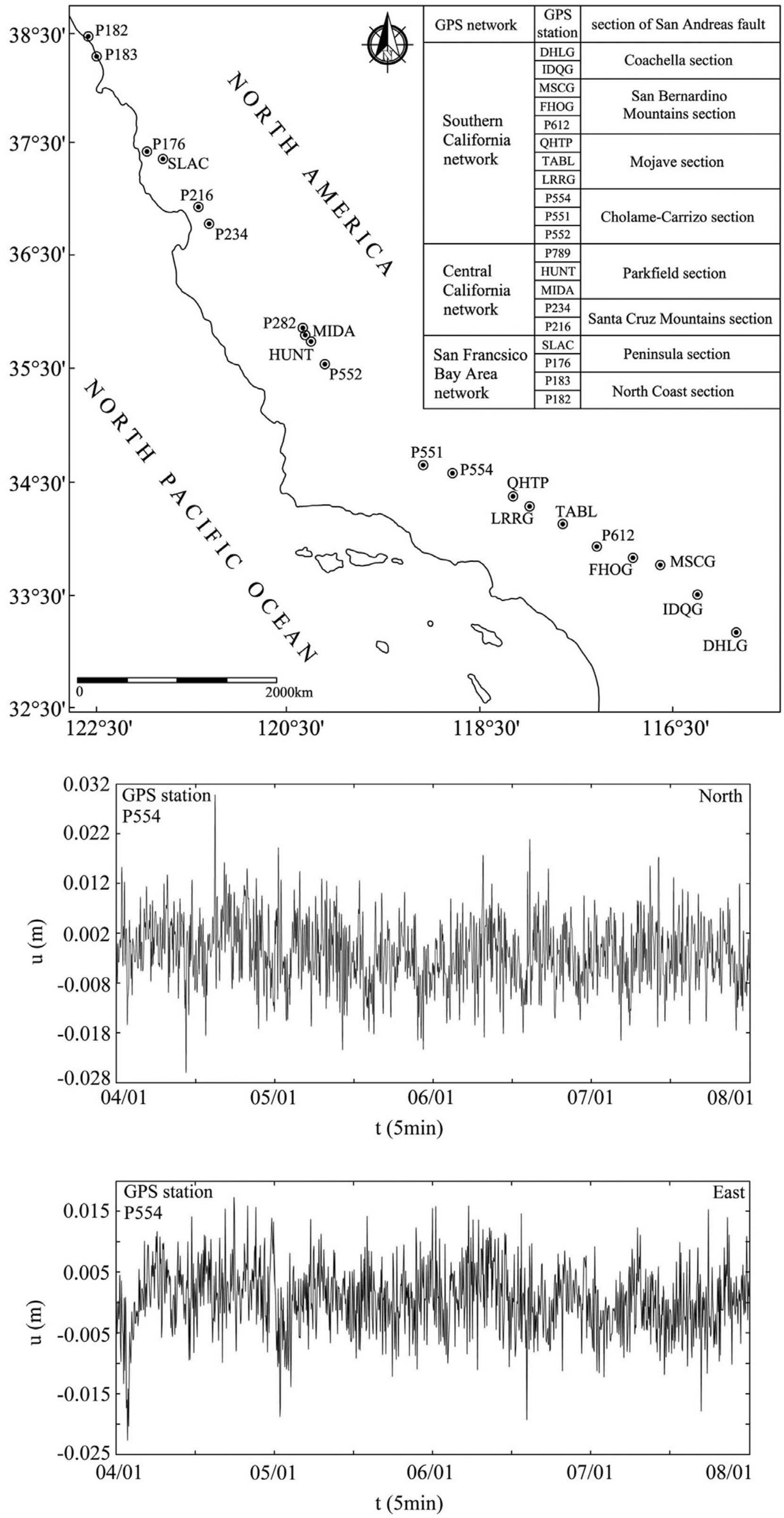

Fig. 1. Uniformly distributed GPS stations along a San Andreas fault, whose measurements are examined in present paper (upper panel). Example of recorded north (middle panel) and east (lower panel) horizontal crustal deformation in the period 04/01/2015–08/01/2015 at a GPS station P554. Qualitatively similar time series are recorded at other GPS stations.

significance level of $\alpha = 0.95$ when confirming or rejecting a null hypothesis, which means that for a single-sided test we have to generate $[1/(1-\alpha)]-1$ surrogates for the original data. Therefore, 19 surrogates are generated by randomly shuffling the data (without repetition), thus yielding surrogates with exactly the same distribution yet independent construction. Surrogates are generated using Matlab toolkit MATS [31]. In order to test the null hypothesis, zeroth-order prediction error is calculated for the original recording (γ_0) and for each of the 19 generated surrogates (γ) according to the algorithm suggested by Kantz and Schreiber [32]. If $\gamma_0 < \gamma$, then a null hypothesis can be rejected. On the other hand, if $\gamma_0 > \gamma$ at any instance of the test, we could not reject null hypothesis. Prediction errors were calculated by embedding each time series into the phase space with embedding dimension $m \in [1,5]$ and embedding delay $\tau \in [1,5]$. In particular, embedding dimension was determined using the symplectic geometry method [33], while mutual information method [34] was applied for embedding delay. Neighbors for prediction were sought among those points that were inside 5% of the maximal distance to the reference, excluding the effect of in-time neighbors.

Results of the performed analysis indicate that temporal changes of crustal deformation in horizontal direction belong to a class of random temporally uncorrelated series. Apparently, zeroth-order prediction error for the original data γ_0 for all the examined GPS measurements is well within the prediction error of the randomly shuffled series γ irrespective of prediction step n for all generated surrogates, except for the first few prediction steps, which we consider as a transient feature (Fig. 2). Relying on these results, further analysis is conducted by assuming that such behavior arises from the effect of incoherent seismic noise, modeled as independent Wiener process.

3. Model setup

In present paper, earthquake fault motion is examined by analysis of dimensionless spring-slider model with N units, whose dynamics is described by the following set of stochastic delay differential equations (SDDEs):

$$\begin{aligned}\dot{U}_{1i}(t) &= U_{2i}(t)\\ dU_{2i}(t) &= \left\{-U_{1i}(t) + \Phi(U_{2i}+\nu) - \Phi(\nu) + \frac{K}{N}\sum_{j=1}^{N}\left[U_{1j}(t-\tau) - U_{1i}(t)\right]\right\}dt + \sqrt{2D}dW_i,\end{aligned} \tag{1}$$

where U_{1i} and U_{2i} represent displacement and velocity of the ith block, respectively, K is constant of spring connecting the blocks, Φ stands for the friction force, τ is time delay and ν is a nondimensional pulling background velocity. Terms $\sqrt{2D}dW_i$ represent stochastic increments of independent Wiener process, i.e. dW_i satisfy:

$$E(dW_i) = 0,\ E\left(dW_i dW_j\right) = \delta_{ij}dt \tag{2}$$

where $E()$ denotes the expectation over many realizations of the stochastic process and D is intensity of additive local noise. Each of $i = 1,2,\dots,N$ units in (1) is coupled with each other unit.In present case, we examine system of 100 units ($N = 100$). In present analysis, values of time delay τ and coupling strength K are chosen to be equal for all the blocks in system (1), which is the limit case of homogeneous conditions along the fault. Also, equal values of coupling strength and time delay could be observed as mean values of these parameters in a multi-block system.

One should note that friction force Φ in (1) is given in general form due to simplicity. In particular, it is assumed to be only rate-dependent:

$$\Phi(V) = -(\mu_0 + a\ln(V)), \tag{3}$$

where V is the general notion for the friction arguments in (1). This type of friction resembles of the friction force already proposed by Scholz [35], only without the state dependent term, which is incorporated in (1) by introducing the time delay τ. In (3), μ_0 is a steady-state friction (whose value could be assumed arbitrarily large in order to secure the proper action of friction force), while a represent a material property which depends on different temperature and pressure conditions. Such prominent dependence of friction on slip rate is qualitatively supported by the recent laboratory findings, which indicate more complex nature of fault friction, but still strongly dependent on slip rate [36,37]. One should note that Eq. (1) is derived according to the previously proposed model [38]. Details of derivation are given in the Appendix.

From the viewpoint of nonlinear dynamics, detailed mathematical model of fault motion (1) involves an extremely large system of nonlinear stochastic delay differential equations (SDDEs), making its analysis impossible without more or less severe approximations. In order to be able to analyze dynamics of system (1), we need to derive its deterministic approximation, which will sufficiently accurately describe its dynamics, and will enable local bifurcation analysis. It is our goal to study some aspects of an approximation determined by only five deterministic delay differential equations (DDEs) of a fault motion model described by many-component SDDEs. For this purpose, we apply the method of mean-field approximation, which is based on a set of approximations that replace a many component system by a simpler system described by a small number of average macroscopic properties [39]. The attempts at providing a reduced description instead of using the complete set of equations for every constituent of the population have a particularly long history within neuroscience [40–43]. Similar approach has also been applied in the area of seismology, primarily for analyzing the dynamics of earthquake fault models, such as cellular automata or spring-slider model. For instance, Dahmen et al. [44] analyzed a heterogeneous fault system as an array of discrete cells in a two-dimensional plane, with elastic coupling between cells in the mean-field approximation. Results of their research imply that calculated exponents for the power-law earthquake distributions and the

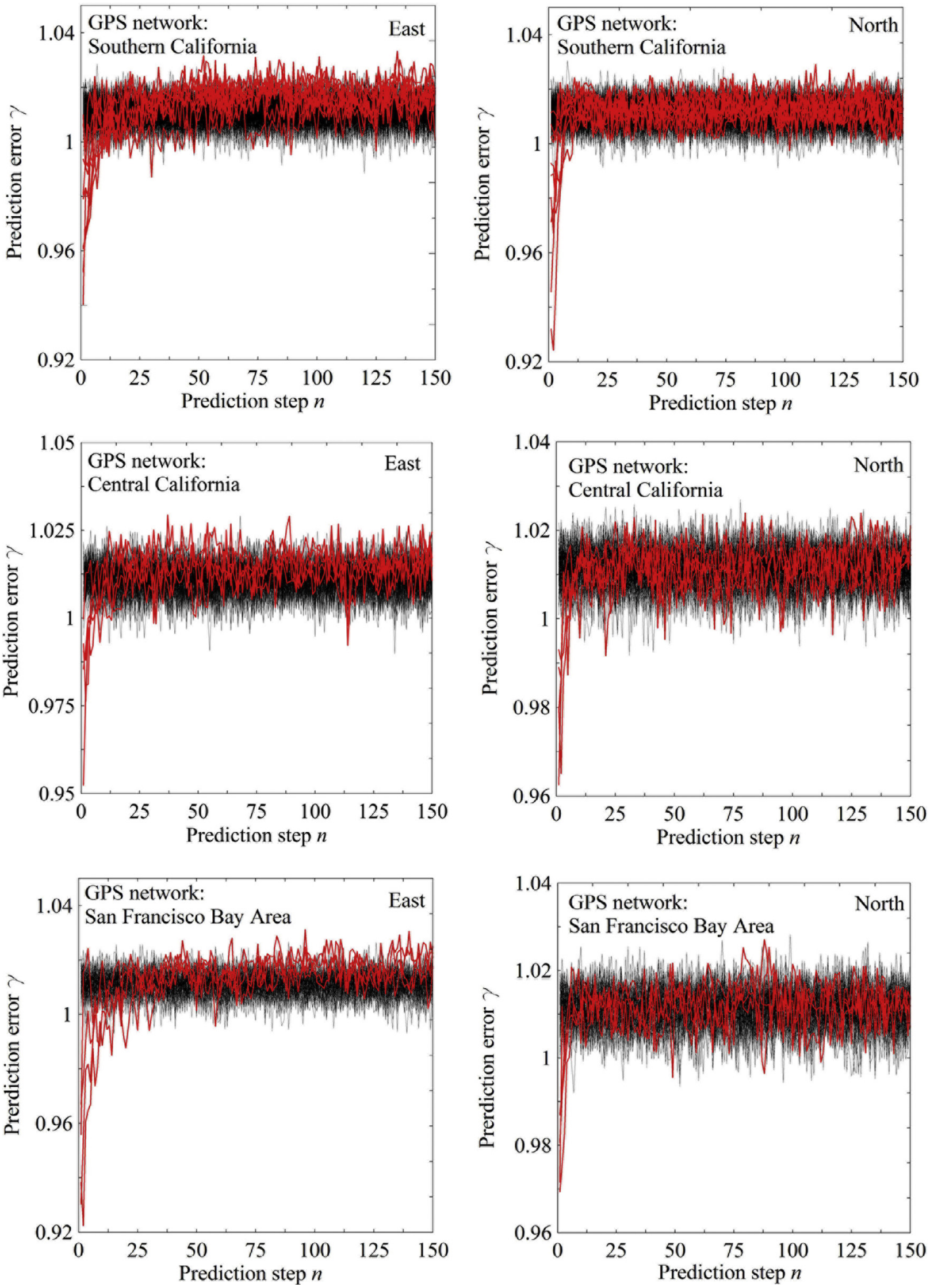

Fig. 2. Surrogate data test for the null hypothesis that data are independent random numbers drawn from some fixed but unknown distribution. Black lines indicate zeroth-order prediction errors for the surrogates (γ), while red lines denote prediction errors for the original recordings (γ_0) as a function of prediction steps n. Results in left and right panels pertain to the measurements in horizontal north and east direction, respectively, for all recording stations belonging to the specified GPS networks. It is clear that except for the first few prediction steps, γ_0 is well within distribution of γ, which makes it impossible to reject the null hypothesis. (For interpretation of the references to color in this figure legend, the reader is referred to the web version of this article.)

divergence of the cutoff length scale for the mean-field model can be expected to apply to models with realistic interactions, with possible logarithmic corrections. As for the spring-slider models, Xia et al. [7] found a mean-field spinodal critical point in a BK model with long-range stress transfer between the blocks as in the long-range cellular automata models. Moreover, some previous studies [45,46] indicated that natural earthquake fault systems are effectively ergodic and mean-field for significant periods of time.

Within present research, method of mean-field approximation gave the final approximated model (1) in the following form:

$$\begin{aligned}
&\dot{m}_{U_1}(t) = m_{U_2}(t),\\
&\dot{m}_{U_2}(t) = -m_{U_1}(t) + a\ln\nu - a\ln(m_{U_2}+\nu) + \frac{a}{2}\frac{1}{(m_{U_2}+\nu)^2}s_{U_2} + \frac{a}{4}\frac{1}{(m_{U_2}+\nu)^4}3s_{U_2}^2 +\\
&\qquad + K[m_{U_1}(t-\tau) - m_{U_1}(t)],\\
&\frac{1}{2}\dot{s}_{U_1}(t) = s_{U_1U_2}\\
&\frac{1}{2}\dot{s}_{U_2}(t) = s_{U_2}\left[-\frac{a}{(m_{U_2}+\nu)} - \frac{a}{(m_{U_2}+\nu)^3}s_{U_2}\right] - (K+1)s_{U_1U_2} + D,\\
&\dot{s}_{U_1U_2} = -s_{U_1U_2}\left[\frac{a}{(m_{U_2}+\nu)} + \frac{a}{(m_{U_2}+\nu)^3}s_{U_2}\right] - (K+1)s_{U_1} + s_{U_2}(t)
\end{aligned} \tag{4}$$

Detailed derivation of model (4) is given in the Appendix. Further on, we shall proceed with a standard local bifurcation analysis of the system (4) in the vicinity of the equilibrium point.

4. Local bifurcation analysis

Local bifurcation analysis of the approximated model (4) is conducted numerically using DDE-BIFTOOL in Matlab, which comprises a collection of adaptable Matlab routines suitable for the numerical bifurcation analysis of systems of DDEs [47]. The obtained results indicate a transition from equilibrium state to periodic oscillations for certain parameter values, as it is shown in Fig. 3. These dynamical states for mean-field model (4), i.e. 5 deterministic equations (left panel at Fig. 4) correspond well to the behavior of the starting system (1), i.e. 200 stochastic equations (right panel at Fig. 4). In particular,

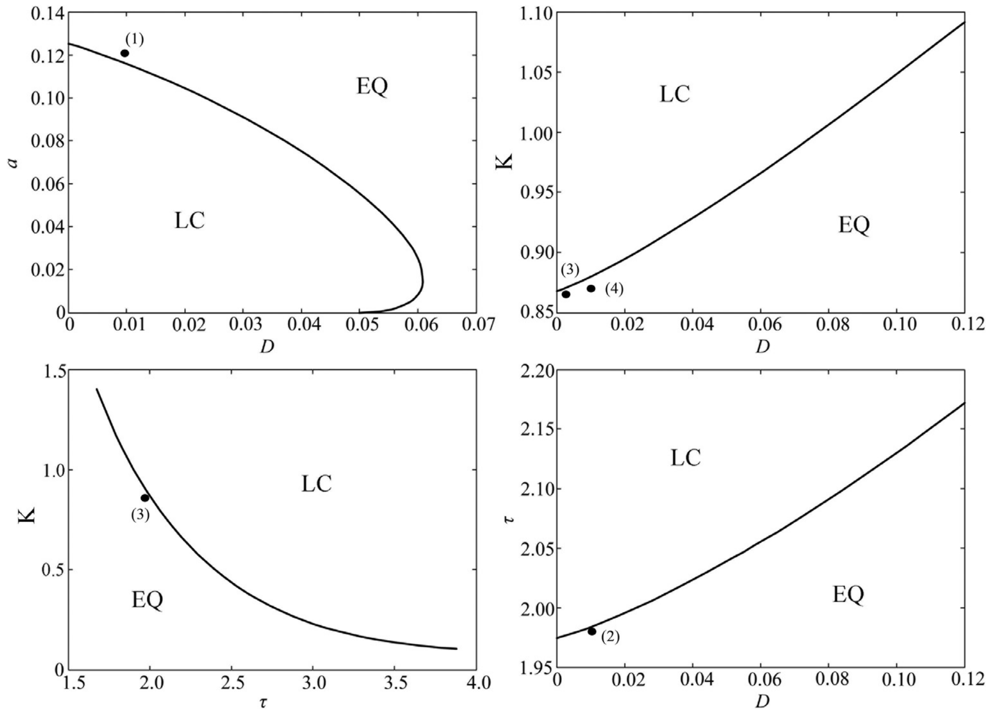

Fig. 3. Parameter domains (a,D), (K,D), (K,τ) and (τ,D) admitting equilibrium state (EQ) or periodic oscillations (LC) of the mean-field approximated model (4). For a given parameter domain, other parameters are held constant at the following values: $K=0.9$, $\nu=1.2$, $D=0.001$, $\tau=2$, $a=0.1$. Starting system (1), due to stochastic effect of included seismic noise in both cases exhibit fluctuations, which are smaller than assumed noise amplitude in EQ region, and are periodic with nearly constant amplitude in LC region. Points (1)–(4) denote the cases for which the event distribution is determined and shown in Fig. 6.

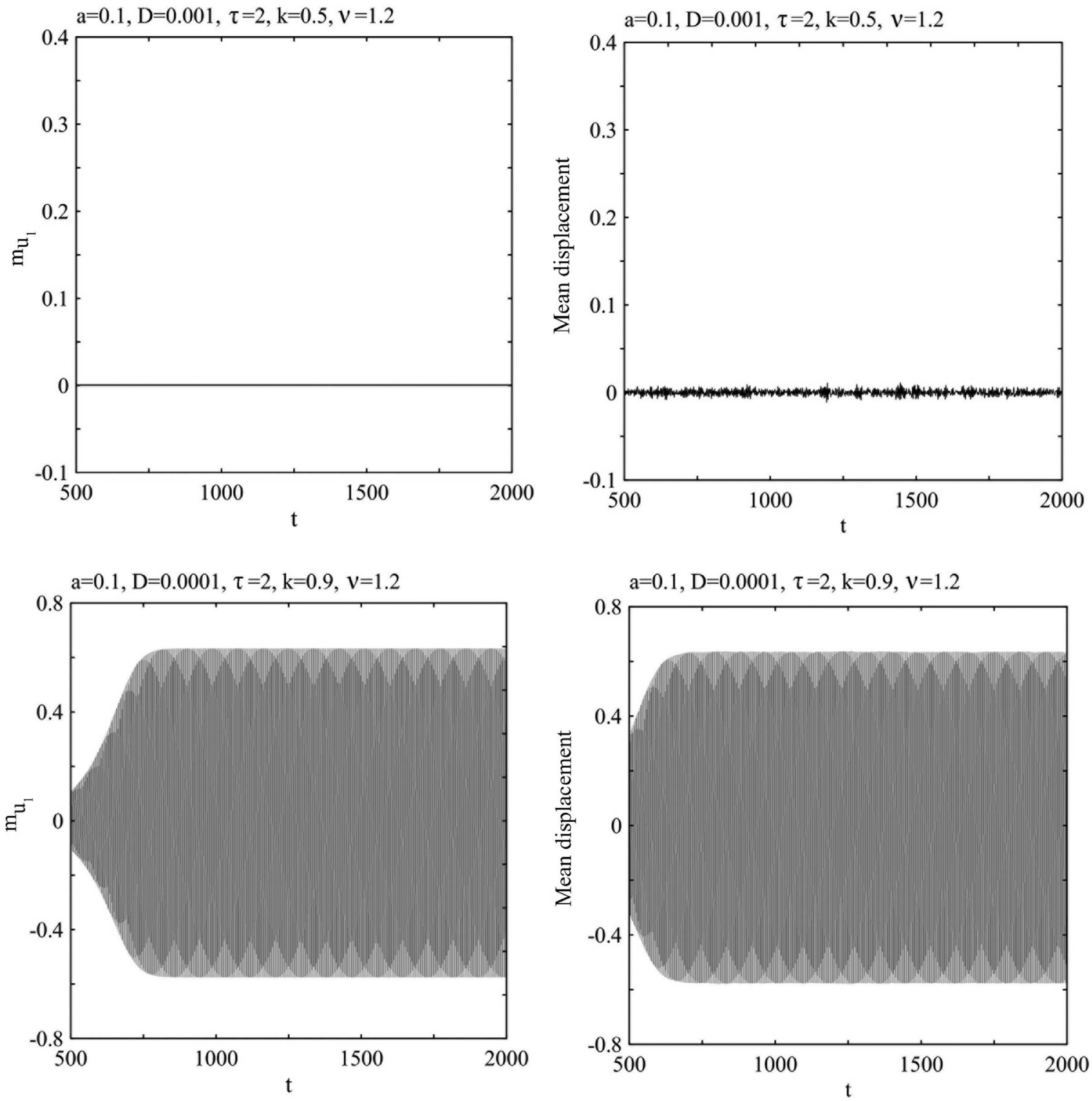

Fig. 4. Time series of approximated mean-field displacements (left panels) and corresponding mean displacements of 100 blocks (right panels). Parameter values are conveniently chosen for equilibrium state and periodic oscillations. It is clear that mean-field model (4) in a sufficiently accurate way describes dynamics of the starting model (1), marking in that way expected position of stochastic bifurcation curves for the starting system (1). Frequency of oscillations for both the starting stochastic model and its mean-field approximation is the same ($f = 0.33$).

performed numerical analysis showed that qualitatively similar dynamics is observed for both the starting stochastic system of N blocks (1) and its mean-field approximation (4). One should note that in Fig. 4 we only show time series of a mean displacement for the starting system (1) and mean-field approximated model (4), since displacement magnitude is directly proportional to earthquake magnitude. Corresponding time series for mean velocity of systems (1) and (4) are qualitatively similar. Also, it should be emphasized that negative values of displacement and velocity are the consequence of the coordinate transformation, where the system is constantly moving around the stationary value $\nu = 1.2$. It should be noted that for cases $U_2 < 0$, friction force acts in opposite direction, i.e. in both cases (positive and negative values of velocity), it opposes the displacement of the block.

Equilibrium state for the starting model (1) is represented by small fluctuations around the constant zero value of a mean-field approximated displacement for a mean-fied model (4). On the other hand, when bifurcation curve is crossed (e.g. in diagram K–τ), oscillation frequencies are the same for both the starting model (1) and approximated system (4), while amplitude could be slightly different due to effect of the introduced random seismic noise in the stochastic model (1). It should be noted that equilibrium state and periodic oscillations are clearly captured only in K–τ diagram. Bifurcation

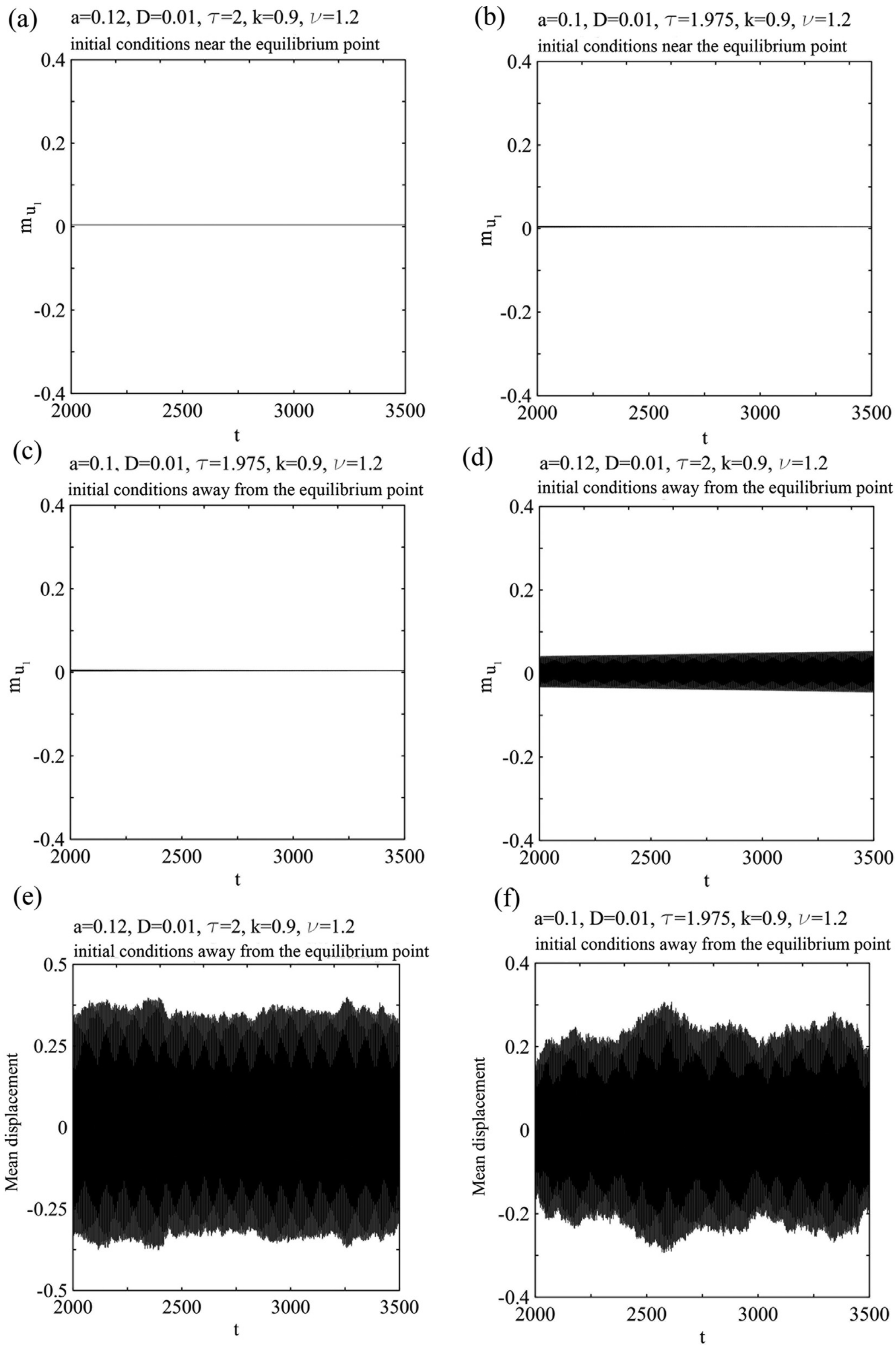

Fig. 5. (a–d) Time series of mean-field displacement in an approximated model (4) for initial conditions away from and near the equilibrium point and for different values of material property a and time delay τ prior the bifurcation. (e, f) Time series of mean displacement of 100 blocks in a starting non-approximated system (1) for initial conditions away from the equilibrium point and for different values of material property a and time delay τ prior the bifurcation. Qualitatively similar time series for starting system (1) are obtained for the same parameter values, but for initial conditions near the equilibrium point.

curves in other diagrams, where parameters a, τ and K are given as function of D, are captured only for the mean-field approximated model (4). These bifurcations in the real starting model (1) are captured only as significantly higher fluctuations of stochastic system when bifurcation curve is crossed.

In this way, we confirmed that mean-field approximated model (1) describes the dynamics of the starting model (1) accurately enough, so the obtained bifurcation curves in general correspond to bifurcations of the original system. From the seismological viewpoint, different dynamical states correspond to different regimes of aseismic motion, i.e. equilibrium state corresponds to the state when there is no movement along the fault or steady sliding along the fault in the original system (1A), while the periodic oscillatory motion denotes the aseismic creep along the fault, which is well documented in real conditions in the Earth's crust [48,49].

One should note that a more detailed analysis of the observed dynamics imply the following. In dependence on initial conditions, for parameter values prior to bifurcation, mean-field approximated model (4) could be in EQ regime or within

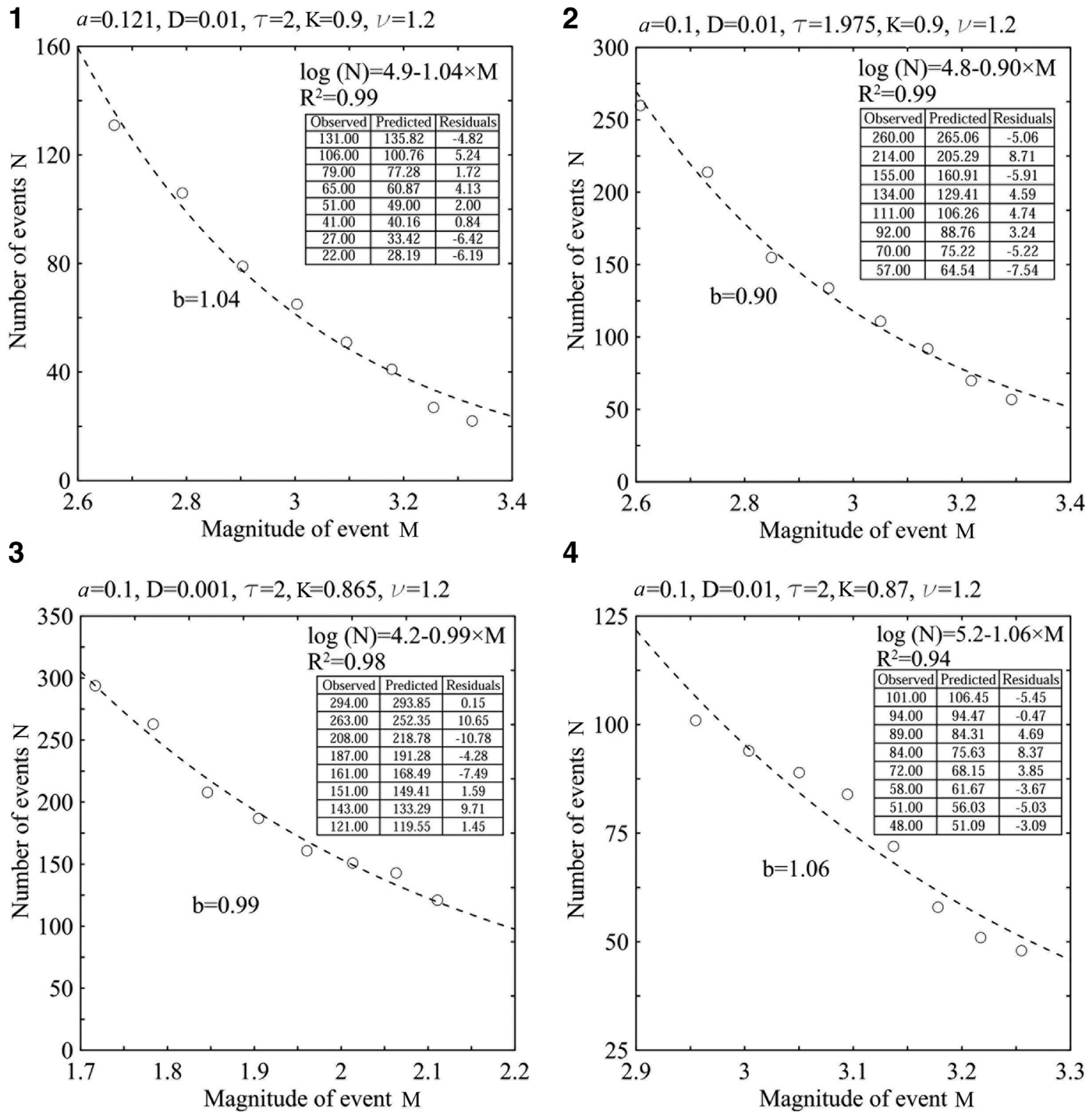

Fig. 6. Examples of power-law behavior of system (1) away from the equilibrium point in a bi-stable regime near the bifurcation curves, for the points (1)–(4) in Fig. 3. It is clear that for different parameter values magnitude–frequency distribution follows the Gutenberg–Richter law with satisfying statistical accuracy, while the corresponding b-value is in the range of real observed data. The lower cut-off was chosen so as to exclude displacements below or equal to the introduced seismic noise, as well as displacement for which event magnitude $M = 0$. Furthermore, for each example, ratio of velocity sums of all blocks to the introduced noise level is at least 10^2, which qualitatively corresponds to the real observed values.

a so-called “bi-stable regime”. When initial conditions are set near the equilibrium point, mean-field model (4) is in EQ regime, regardless of the parameter values (before the bifurcation occurs, Fig. 5a and b). On the other hand, if initial conditions are set away from the equilibrium point, mean-field model (4) could be in EQ regime (Fig. 5c) or could exhibit oscillatory behavior due to effect of global bifurcation depending on the parameter values prior to local bifurcation (Fig. 5d). In a starting stochastic system of N blocks (1), impact of global bifurcation reveals in high amplitude fluctuations above the introduced noise level (Fig. 5f). However, such fluctuations in system (1) could also arise due to sole effect of the introduced random seismic noise (Fig. 5e), if the system (4) is close enough to bifurcation curve, regardless of the initial conditions.

In summary, on the basis of the conducted bifurcation analysis, two main conclusions could be drawn. First of all, mean-field model (4) sufficiently well describes dynamics of the starting model (1), which is indicated by qualitatively the same dynamical behavior below and above the obtained bifurcation curves. Secondly, irregular behavior of the starting model (1) imply two possible scenarios: either the effect of introduced noise induces the possible occurrence of stochastic bifurcation or there exists another basin of attraction of some global attractor in parallel to basin of attraction of the equilibrium point.

5. Macroseismic implications

From the viewpoint of seismology, performed bifurcation analysis indicates that earthquakes could be expected to occur only in a bi-stable dynamical regime in the vicinity of a bifurcation curve provided that initial conditions along the fault are far from the equilibrium state (the case of active fault). In particular, irregular oscillations with amplitude higher than assumed noise level arise only for this regime, as an effect of either the introduced noise or the global attractor. Small fluctuations of system (1) well below the bifurcation curve, which correspond to equilibrium state, cannot be treated as relevant for real seismic events, since their amplitudes are significantly lower than the introduced noise level. On the other hand, regular periodic oscillations of the starting system (1) above the bifurcation curve could hardly be expected to occur in real conditions, since regular periodic recurrence of seismic events has rarely been observed along a single fault. In particular, periodic occurrence of earthquakes is captured in the real conditions only for the strongest earthquakes at certain locations in the Earth’s crust, like Nankai seismic area [50]. Nevertheless, if we take into account all earthquakes recorded in a single area, than their occurrence will certainly be aperiodic. Therefore, we could treat periodic oscillations also as an example of aseismic creep, which is more frequent case in the reality [48,49].

In order to verify that a starting model (1) in a bi-stable dynamical regime exhibits dynamics which is relevant for the real observed seismicity, we analyze the statistical distribution of events for different time series of displacement sums near the bifurcation curves (Fig. 6). In this case, magnitude of an event is typically defined as a natural logarithm of displacement sums for all blocks [16], while an event is defined as a peak (local maximum) of mean displacement of system (1) above a certain threshold. Introduced noise level is conveniently chosen so as to obtain results which are comparable with the real observed data. In particular, for the lower cut-off we chose those sums whose magnitude is equal to $M = 0$, excluding in that way very weak earthquakes which are induced only by small displacements along the observed fault. Also, average ratio of velocity sums to the introduced noise is at least 10^2, which is typically reported as a lower threshold for this ratio in real conditions.

Performed statistical analysis indicated that distribution of observed event magnitudes for a certain time range, neglecting the transients, follows the Gutenberg–Richter power law with satisfying statistical accuracy (high values of R^2 and low residual sum of squares) and with the b-value in the range [0.90–1.06], which corresponds well to the real observed data.

6. Conclusion

In present paper, we analyzed stochastic model of fault motion with included effect of seismic noise and time delay. Introduction of seismic noise was justified by surrogate data analysis of ground deformation near San Andreas fault system, which showed that fault movement could be treated as a random process, probably due to the impact of incoherent seismic noise. On the other hand, delayed interaction of blocks within a fault system was also found in the original work of Burridge and Knopoff [1] and it was implied by the real observed data.

Dynamics of starting model, which consists of 100 blocks, is examined using mean-field approach, which enabled us to detect the possible occurrence of deterministic bifurcations. In particular, instead of 200 stochastic delay differential equations, mean-field approach provided five delay differential equations, which sufficiently accurate describe the behavior of the starting system. The obtained results indicate that a bifurcation from equilibrium point to limit cycle occurs for a certain parameter range. Long-period aperiodic irregular oscillations also arise, either due to the introduced seismic noise or they occur under the impact of some global attractor. Either way, these long-period oscillations are shown to obey power-law behavior, with the parameter values which are comparable to the real observed data.

If one compares the performed research and obtained results with the previous studies on the same topic, several novelties could be singled out. First of all, seismic noise and delayed interaction among different fault segments (interacting blocks of the model), as existing natural factors, are for the first time introduced in the examined model. Secondly, method of mean-field approximation is for the first time applied in the analysis of dynamics of a spring-block model, providing sufficiently accurate results. Moreover, it is shown for the first time that irregular mean displacement of a whole fault near the transition from equilibrium state (EQ regime) to aseismic creep (LC regime) could occur either due to sole effect of seismic noise or under the impact of seismic noise in the presence of local and global attractor. This is contrast with previous studies, which commonly claimed that irregular displacement of a fault, i.e. seismic motion, represents an example of deterministic chaos [21,22,38].

In conclusion, performed research set a solid base for future studies for two main reasons. Firstly, it is shown that stochastic model of fault motion is justified from the viewpoint of seismology, relying on the results of real observed data and surrogate data testing. Secondly, irregular oscillations near the bifurcation curve, which resemble of stick-slip motion, are confirmed to obey power-law behavior. On the basis of these main results, further research should focus on interaction of blocks within the model, by comparing individual and collective behavior. Moreover, interaction of blocks in a two-dimensional plane would certainly bring new dynamical features which could have significant implications from seismological viewpoint.

Acknowledgments

This research has been partly supported by the Ministry of Education, Science and Technological development of the Republic of Serbia, Contract nos. 171015 and 176016.

Appendix

Model derivation

Present research on earthquake fault motion is based on the analysis of non-dimensional mono-block model, originally suggested in [38]:

$$\ddot{U}(t) = -U(t) + \Phi\big(\dot{U}(t)\big) + \nu t, \tag{1A}$$

where variable U represents the block displacement, $\dot{U}$ is the velocity of the block (defined in the standing reference frame), $\ddot{U}$ is the block acceleration, ν is dimensionless pulling speed, and t is time variable. Friction force Φ is assumed to be only rate-dependent. The unstable equilibrium around which the orbits of block move in phase space is given in the following way:

$$U_e(t) = \nu t + \Phi(\nu), \tag{2A}$$

which is determined by setting $\ddot{U} = 0$ and $\dot{U} = \nu$ in (1A).

From (1A), one can write:

$$\begin{aligned} \dot{U}_1(t) &= U_2(t) \\ \dot{U}_2(t) &= -U_1(t) + \Phi(U_2(t)) + \nu t, \end{aligned} \tag{3A}$$

where U_1 and U_2 denote displacement and velocity of a single block, respectively.

Using the following coordinate transformation:

$$\begin{aligned} U_{1new}(t) &= U_1 - U_e(t) = U_1(t) - (\nu t + \Phi(\nu)), \\ U_{2new}(t) &= U_2(t) - \nu, \end{aligned} \tag{4A}$$

after which we return to old notation, one could get the following system of equation for the motion of a single block:

$$\begin{aligned} \dot{U}_1(t) &= U_2(t) \\ \dot{U}_2(t) &= -U_1(t) + \Phi(U_2(t) + \nu) - \Phi(\nu). \end{aligned} \tag{5A}$$

Starting from (5A) one can derive the spring-slider model of N interconnected blocks given as system of Eq. (1) in Section 3.

Mean-field approximation

By deriving the Taylor expansion of $\Phi(U_2(t)+\nu)$ in the vicinity of the mean values $(\langle U_1\rangle, \langle U_2\rangle) = (\lim_{N\to\infty}\frac{1}{N}\sum_{i=1}^{N} U_{1i}(t), \lim_{N\to\infty}\frac{1}{N}\sum_{i=1}^{N} U_{2i}(t)) = (m_{U_1}, m_{U_2})$ system (1), in the thermodynamic limit, for $N\to\infty$, becomes:

$$\begin{aligned} dU_{1i}(t) &= U_{2i}(t)dt \\ dU_{2i}(t) &= \{-U_{1i}(t) + \Phi(m_{U_2}+\nu) - \Phi(\nu) + \frac{1}{1!}[\Phi'(m_{U_2}+\nu)][U_2(t) - m_{U_2}] + \\ &\quad + \frac{1}{2!}[\Phi''(m_{U_2}+\nu)][U_2(t) - m_{U_2}]^2 + \frac{1}{3!}[\Phi'''(m_{U_2}+\nu)][U_2(t) - m_{U_2}]^3 + \\ &\quad + \frac{1}{4!}[\Phi^{(4)}(m_{U_2}+\nu)][U_2(t) - m_{U_2}]^4 + K[m_{U_1}(t-\tau) - U_1(t)]\}dt + \sqrt{2D}dW_i. \end{aligned} \tag{1B}$$

In order to derive mean-field approximate dynamical equations for starting system (1) in the main text, we shall first suppose that: (a) dynamics is such that the distributions of U_{1i} and U_{2i} are Gaussian and (b) for large N the average over local random variables is given by the expectation with respect to the corresponding distribution, as in [39]. In the limit $N\to\infty$, the last assumption is expected to become equality, implied by the strong law of large numbers [51]. In the mean-field approach it is commonly assumed that (b) is approximately true even for finite but large N despite the non-zero interaction between the local random variables. The first assumption should be expected to be true when the noise intensity is small, i.e. $D \ll 1$ [52,53]. With these assumptions the system (1B) of N SDDEs can be reduced to five DDEs for the macroscopic variables $m_{U_1}(t), m_{U_2}(t)$ and the second order cumulants.

Following the procedure from Burić et al. [39], starting system (1B) of N SDDEs is reduced to the system of only five deterministic DDEs for the global variables and global centered moments:

$$m_{U_1}(t) = \langle U_1(t)\rangle,\ m_{U_2}(t) = \langle U_2(t)\rangle,\ s_{U_1}(t) = \left\langle n_{U_1}^2(t)\right\rangle,\ s_{U_2}(t) = \left\langle n_{U_2}^2(t)\right\rangle,\ s_{U_1U_2}(t) = \langle n_{U_2}\cdot n_{U_1}\rangle, \tag{2B}$$

where $n_{U_j}(t) = m_{U_j}(t) - U_{ji}(t)$, $j=1,2$.

The final mean-field approximated model with the general form of friction term Φ is given in the following way:

$$\begin{aligned}
\dot m_{U_1}(t) &= m_{U_2}(t),\\
\dot m_{U_2}(t) &= -m_{U_1}(t) + \Phi(m_{U_2}+\nu) - \Phi(\nu) + \frac{1}{2}\left[\Phi''(m_{U_2}+\nu)\right]s_{U_2} + \frac{1}{24}\left[\Phi^{(4)}(m_{U_2}+\nu)\right]3s_{U_2}^2 + \\
&\quad + K[m_{U_1}(t-\tau) - m_{U_1}(t)],\\
\frac{1}{2}\dot s_{U_1}(t) &= s_{U_1U_2}\\
\frac{1}{2}\dot s_{U_2}(t) &= s_{U_2}\left[\Phi'(m_{U_2}+\nu) + \frac{1}{2}\Phi'''(m_{U_2}+\nu)s_{U_2}\right] - (K+1)s_{U_1U_2} + D,\\
\dot s_{U_1U_2} &= s_{U_1U_2}\left[\Phi'(m_{U_2}+\nu) + \frac{1}{2}\Phi'''(m_{U_2}+\nu)s_{U_2}\right] - (K+1)s_{U_1} + s_{U_2}(t)
\end{aligned} \tag{3B}$$

The final form of (3B) with included rate-dependent friction term is given in the main text as system (4).

References

[1] Burridge R, Knopoff L. Model and theoretical seismicity. B Seismol Soc Am 1967;57:341–71.
[2] Carlson J, Langer J. Mechanical model of an earthquake fault. Phys Rev A 1989;40:6470–84.
[3] Carlson JM, Langer JS, Shaw BE, Tang C. Intrinsic properties of a Burridge–Knopoff model of an earthquake fault. Phys Rev A 1991;44:884–97.
[4] Schmittbuhl J, Vilotte J, Roux S. A dissipation-based analysis of an earthquake fault model. J Geophys Res 1996;101 27,741–64.
[5] Hainzl S, Zoller G, Kurths J. Self-organized criticality model for earthquakes: quiescence, foreshocks and aftershocks. Int J Bifurc Chaos 1999;9:2249–55.
[6] Mori T, Kawamura H. Simulation study of spatiotemporal correlations of earthquakes as a stick–slip frictional instability. Phys Rev Lett 2005;94:058501–1-4.
[7] Xia J, Gould H, Klein W, Rundle JB. Near-mean-field behavior in the generalized Burridge–Knopoff earthquake model with variable-range stress transfer. Phys Rev E 2008;77:031132–1-11.
[8] Olami Z, Feder HJS, Christensen K. Self-organized criticality in a continuous, nonconservative cellular automaton modeling earthquakes. Phys Rev Lett 1992;68:1244–7.
[9] Knopoff L, Landoni JA, Abinante MS. Dynamical model of an earthquake fault with localization. Phys Rev A 1992;46:7445–9.
[10] Jonsson T, Marinosson SF. Scaling and correlation functions in a model of a two-dimensional earthquake fault. Phys Scr 1998;58:282–8.
[11] De Sousa Vieira M. Self-organized criticality in a bulk-driven one-dimensional deterministic system. Physica A 2004;344:737–42.
[12] Mori T, Kawamura H. Simulation study of earthquakes based on the two-dimensional Burridge–Knopoff model with long-range interactions. Phys Rev E 2008;77:051123-1–051123-16.
[13] Dieterich JH. Modeling of rock friction: 1; experimental results and constitutive equations. J Geophys Res 1979;84:2161–8.
[14] Ruina A. Slip instability and state variable friction laws. J Geophys Res 1983;88:10359–70.
[15] Perrin G, Rice JR, Zheng G. Self-healing slip pulse on a frictional surface. J Mech Phys Solids 1995;43:1461–95.
[16] Kawamura H, Hatano T, Kato N, Biswas S, Chakrabarti BK. Statistical physics of fracture, friction, and earthquakes. Rev Mod Phys 2012;84:2839–84.
[17] Nussbaum J, Ruina A. A two degree-of-freedom earthquake model with static/dynamic friction. Pure Appl Geophys 1987;5:629–56.
[18] Huang J, Turcotte DL. Chaotic seismic faulting with a mass-spring model and velocity-weakening friction. Pure Appl Geophys 1992;138:569–89.
[19] Field S, Venturi N, Nori F. Marginal stability and chaos in coupled faults modeled by nonlinear circuits. Phys Rev Lett 1995;74:74–8.
[20] Galvanetto U. Some remarks on the two-block symmetric Burridge–Knopoff model. Phys Lett A 2002;293:251–9.
[21] Erickson B, Birnir B, Lavallee D. A model for aperiodicity in earthquakes. Nonlinear Proc Geophys 2008;15:1–12.
[22] Erickson BA, Birnir B, Lavallée D. Periodicity, chaos and localization in a Burridge–Knopoff model of an earthquake with rate-and-state friction. Geophys J Int 2011;187:178–98.
[23] Telford WM, Geldart LP, Sheriff RE. Applied geophysics. 2nd ed. Cambridge: Cambridge University Press; 1990.
[24] Ryabov VB, Correig AM, Urquizu M, Zaikin AA. Microseism oscillations: from deterministic to noise-driven models. Chaos Solitons Fractals 2003;16:195–210.
[25] Sanders CO. Interaction of the San Jacinto and San Andreas fault zones, southern California: triggered earthquake migration and coupled recurrence intervals. Science 1993;260:973–6.
[26] Johnson KM, Segall P. Viscoelastic earthquake cycle models with deep stress-driven creep along the San Andreas fault system. J Geophys Res 2004;109 B10403–1-19.
[27] Franović I, Todorović K, Vasović N, Burić N. Spontaneous formation of synchronization clusters in homogenous neuronal ensembles induced by noise and interaction delays. Phys Rev Lett 2012;108:094101.
[28] Wang JH. Memory effect in $M\geq 7$ earthquakes of Taiwan. J Seismol 2014;18:467–80.
[29] USGS website: http://earthquake.usgs.gov/monitoring/gps/. [accessed 10.01.15].
[30] Perc M, Green AK, Jane Dixon C, Marhl M. Establishing the stochastic nature of intracellular calcium oscillations from experimental data. Biophys Chem 2008;132:33–8.

[31] Kugiumtzis D, Tsimpiris A. Measures of analysis of time series (MATS): a MATLAB toolkit for computation of multiple measures on time series data bases. J Stat Softw 2010;33:1–30.
[32] Kantz H, Schreiber T. Nonlinear time series analysis. Cambridge: Cambridge University Press; 2004.
[33] Lei M, Wang Z, Feng Z. A method of embedding dimension estimation based on symplectic geometry. Phys Lett A 2002;303:179–89.
[34] Fraser A, Swinney H. Independent coordinates for strange attractors from mutual information. Phys Rev A 1986;33:1134–40.
[35] Scholz CH. Earthquakes and friction laws. Nature 1998;391:37–42.
[36] Sone H, Shimamoto T. Frictional resistance of faults during accelerating and decelerating earthquake slip. Nat Geosci 2009;2:705–8.
[37] Lapusta N. The roller coaster of fault friction. Nat Geosci 2009;2:676–7.
[38] De Sousa Vieira M. Chaos and synchronized chaos in an earthquake model. Phys Rev Lett 1999;82:201–4.
[39] Burić N, Ranković D, Todorović K, Vasović N. Mean field approximation for noisy delay coupled excitable neurons. Physica A 2010;389:3956–64.
[40] Hasegawa H. Stochastic bifurcation in FitzHugh Nagumo ensembles subjected to additive and/or multiplicative noises. Physica D 2008;237:137–55.
[41] Lindner B, Garcia-Ojalvob J, Neimand A, Schimansky-Geiere L. Effects of noise in excitable systems. Phys Rep 2004;392:321–4.
[42] Stefanescu RA, Jirsa VK. A low dimensional description of globally coupled heterogeneous neural networks of excitatory and inhibitory neurons. PLoS Biol 2008;4:1–17.
[43] Franović I, Todorović K, Vasović N, Burić N. Mean-field approximation of two coupled populations of excitable units. Phys Rev E 2013;87:012922-1-13.
[44] Dahmen K, Ertas D, Ben-Zion Y. Gutenberg–Richter and characteristic earthquake behavior in simple mean-field models of heterogeneous faults. Phys Rev E 2008;58:1494–501.
[45] Ferguson CD, Klein W, Rundle JB. Spinodals, scaling, and ergodicity in a threshold model with long-range stress transfer. Phys Rev E 1999;60:1359–74.
[46] Tiampo KF, Rundle JB, Klein W, Holliday J, Sa Martins JS, Ferguson CD. Ergodicity in natural earthquake fault networks. Phys Rev E 2007;75:066107-1–066107-16.
[47] Engelborghs K, Luzyanina T, Samaey G. DDE-BIFTOOL v. 2.00: a Matlab package for bifurcation analysis of delay differential equations. Leuven, Belgium: Department of Computer Science, K.U. Leuven; 2000.
[48] Galehouse J, Lienkaemper J. Inferences drawn from two decades of alinement array measurements of creep on faults in the San Francisco Bay Region. Bull Seismol Soc Am 2003;93:2415–33.
[49] Lienkaemper JJ, McFarland FS, Simpson RW, Bilham RG, Ponce DA, Boatwright JJ, et al. Long-term creep rates on the Hayward fault: evidence for controls on the size and frequency of large earthquakes. Bull Seismol Soc Am 2012;102:31–41.
[50] Parsons T, Console R, Falcone G, Muru M, Yamashina K. Comparison of characteristic and Gutenberg–Richter models for time-dependent$M \geq 7.9$ earthquake probability in the Nankai–Tokai subduction zone, Japan. Geophys J Int 2012;190:1673–88.
[51] Arnold L. Random dynamical systems. Berlin: Springer-Verlag; 1998.
[52] Tanabe S, Pakdaman K. Dynamics of moments of FitzHugh–Nagumo neuronal models and stochastic bifurcations. Phys Rev E 2001;63:031911.
[53] Zaks MA, Siler X, Schimansky-Geier L, Neiman AB. Noise induced complexity: from subthreshold oscillations to spiking in coupled excitable systems. Chaos 2005;15:026117.